Acta Biochim Biophys Sin 2026, 58(9): 1–16
https://cstr.cn/32197.14.abbs.2026112
https://doi.org/10.3724/abbs.2026112
Original Article

Original Article

EZH2-dependent STAT3 stabilization drives pomalidomide resistance and is targetable by EZH2 inhibition in multiple myeloma

Xinyuan Zhang[1], Ruijing Hu[2], Kexin Hu[1], Qi Li[1], Linlin Qin[2], Yali Chai[2], Wenzhuo Zhuang[2,*], and Xiaohui Zhang[1,*]

[1]Department of Hematology, the Second Affiliated Hospital of Soochow University, Suzhou 215006, China, and [2]Department of Cell Biology, School of Basic Medical Sciences, Suzhou Medical College of Soochow University, Suzhou 215123, China
*Correspondence address. E-mail: zhxh424@163.com (X.Z.); zhuangwenzhuo@suda.edu.cn (W.Z.)

Received 10 January 2026 Accepted 6 May 2026 Published 26 August 2026

Abstract

Relapsed/refractory multiple myeloma (RRMM) is characterized by high mortality rates and limited survival, with real-world studies reporting substantial mortality and median survival of only a few years after relapse. Immunomodulatory drugs (IMiDs) are a cornerstone of first-line multiple myeloma (MM) therapy, yet resistance remains a major clinical challenge. Resistance to pomalidomide has been attributed to multiple mechanisms, including CRBN downregulation and activation of pro-survival signaling pathways such as NF-κB; however, the contribution of epigenetic regulators, particularly the STAT3EZH-STAT3 axis, remains insufficiently explored. In this study, our analysis of public datasets identifies significant upregulation of enhancer of zeste homolog 2 (EZH2) in RRMM patients together with an association between EZH2 expression and poor prognosis. Using two established pomalidomide-resistant MM models, we confirm elevated EZH2 expression in pomalidomide-resistant MM cell lines, and demonstrate targeting EZH2 via small interfering RNA or the selective inhibitor GSK343 elicits potent anti-myeloma effects in pomalidomide-resistant MM models. Notably, *EZH2* knockdown increases the sensitivity of RRMM cells to pomalidomide, providing a rationale for combining EZH2 inhibition with pomalidomide therapy. Consistent with this observation, GSK343 synergizes with pomalidomide to suppress MM progression both *in vitro* and *in vivo*. To better understand the mechanisms involved, we conduct RNA sequencing and investigate potential mediators of EZH2. We find that EZH2 contributes to pomalidomide resistance through stabilizing STAT3 protein, thereby supporting myeloma cell survival under therapeutic stress. In conclusion, EZH2 inhibition can enhance the therapeutic efficacy of pomalidomide against RRMM, indicating that EZH2 offers a promising target for overcoming drug resistance in MM.

Key words multiple myeloma, EZH2, pomalidomide, drug resistance, GSK343, STAT3

Introduction

Multiple myeloma (MM) is a plasma cell neoplasm marked by the clonal expansion of malignant plasma cells residing in the bone marrow niche which can lead to extensive skeletal destruction, anemia, hypercalcemia, renal dysfunction, and immunodeficiency [1]. Over the past two decades, the advent of immunomodulatory drugs (IMiDs), proteasome inhibitors (PIs), and monoclonal antibodies has revolutionized MM treatment and significantly prolonged patient survival [2]. Among these agents, pomalidomide, a third-generation IMiD, has demonstrated superior efficacy in relapsed/refractory settings and has become an integral component of MM therapy [3]. However, despite these advances, MM remains largely incurable, as most patients eventually experience relapse and develop resistance to pomalidomide. Thus, relapsed and/or refractory MM (RRMM) poses a major clinical challenge [4].

Recent studies have uncovered several molecular mechanisms of pomalidomide resistance, including cereblon (CRBN) downregulation and aberrant activation of the Wnt/β-catenin and nuclear

© The Author(s) 2026. This is an open access article distributed under the terms of the Creative Commons Attribution License (https://creativecommons.org/licenses/by/4.0/).

factor-kappa B (NF-κB) signaling pathways [5-7]. Additionally, alterations in components of the ubiquitin-proteasome system and transcriptional rewiring have been shown to contribute to immune evasion and drug tolerance [8]. These observations help elucidate the complex biology of pomalidomide resistance and highlight potential therapeutic targets for overcoming drug resistance in RRMM [9].

Enhancer of zeste homolog 2 (EZH2) functions as the enzymatic core of the Polycomb repressive complex 2 (PRC2) and catalyzes trimethylation of histone H3 on lysine 27 (H3K27me3), thereby promoting chromatin condensation and repression of gene transcription [10]. As a pivotal epigenetic regulator, EZH2 plays essential roles in cell-cycle regulation, stemness maintenance, and differentiation [11]. Dysregulated levels or functions of EZH2 have been linked to the development and progression of various cancers, including lymphomas, prostate cancer, and breast cancer, in which such changes promote tumor progression, metastasis, and therapy resistance [12]. In multiple myeloma (MM), dysregulated EZH2 is associated with high-risk disease features and poor prognosis [13]. Given the reversible nature of epigenetic modifications, targeting EZH2 with selective inhibitors holds therapeutic promise [14]. Importantly, a recent whole-genome sequencing (WGS) study compared data from relapsed/refractory patients who had sequentially received lenalidomide and pomalidomide with WGS data from 198 newly diagnosed cases and identified EZH2 as a novel candidate driver gene in RRMM [15]. However, the specific mechanism through which EZH2 contributes to the development of pomalidomide resistance remains to be elucidated. Nevertheless, based on the current evidence, EZH2 represents a promising entry point for dissecting the molecular pathways underlying pomalidomide resistance. Elucidating the role of EZH2 in pomalidomide-resistant MM will not only expand our understanding of drug resistance mechanisms but also could provide insights for developing combination strategies to overcome resistance and improve outcomes in RRMM [16].

In the present study, we established and characterized pomalidomide-resistant MM cell lines to explore the molecular mechanisms underlying this resistance [17]. Through transcriptomic analyses, we investigated pathways driving resistance and evaluated potential therapeutic strategies to restore drug sensitivity in MM cells [18].

Materials and Methods

Cell lines and culture conditions

The human multiple myeloma cell lines MM.1S and U266 were purchased from ATCC (Manassas, USA). Cells were cultured in RPMI-1640 medium (12633020; Gibco, Grand Island, USA) containing 10% heat-inactivated fetal bovine serum (FB20015; CLARK, Shanghai, China) and 1% penicillin-streptomycin (1514012; Gibco). All cell cultures were incubated at 37°C in a humidified chamber with 5% carbon dioxide. Cell lines were authenticated using Short Tandem Repeat (STR) analysis performed by Genetic Testing Biotechnology (Suzhou, China) and the submitted profile is an exact match for the following human cell line(s) in the ExPASy (https://www.expasy.org/resources/cellosaurus).

Development of pomalidomide-resistant cell lines

Pomalidomide (P0018-5MG; Sigma-Aldrich, St Louis, USA)-resistant MM cell lines (MM.1S PR and U266 PR) were established by repeated high-dose pulse selection. Parental cells at log phase were exposed to pomalidomide at concentrations approximating the parental half-maximal inhibitory concentration (IC_{50}) which was measured via a microplate reader (Synergy H1; BioTek Instruments, Winooski, USA) for 48 h, after which drug was removed and cells were allowed to recover in drug-free medium. Pulses were repeated weekly until a stable increase in IC_{50} was observed (typically 4–10 cycles). Resistant lines were validated by dose-response assays (BL1055E; BioSharp, Hefei, China) to confirm increased IC_{50} relative to parental cells. Resistant cells were maintained in medium containing a lower maintenance concentration of pomalidomide and aliquots were cryopreserved for downstream experiments. Pomalidomide-resistant cells were maintained in a drug-free medium for a period of two months. During this time, the IC_{50} of pomalidomide was assessed at three independent time points using the CCK-8 assay. In parallel, EZH2 expression levels were evaluated following drug withdrawal (Supplementary Figure S1A).

CCK-8 assay

Cell viability and proliferative capacity were assessed by employing the Cell Counting Kit-8 (BL1055E; BioSharp). In this assay, approximately 5×10^3 multiple myeloma cells were dispensed into each well of 96-well plates and subsequently exposed to pomalidomide (P0018-5MG; Sigma-Aldrich), GSK343 (HY-13500; MCE, Monmouth Junction, USA), MS1943 (HY-133129; MCE) for a duration of 48 h and vehicle controls (DMSO; Sigma-Aldrich) were consistently included in all experiments at equivalent concentrations to exclude potential solvent-related effects. Optical density was recorded at 450 nm using a BioTek microplate spectrophotometer (Synergy H1; BioTek Instruments), and half-maximal inhibitory concentration (IC_{50}) values were estimated from the resulting dose-response relationships.

Western blot analysis

Cells were harvested and lysed using RIPA buffer (P0013C; Beyotime Biotechnology, Shanghai, China) supplemented with protease inhibitor cocktail (P1005; Beyotime Biotechnology). Protein levels were quantified, and equivalent protein samples were resolved by 8%–12% SDS-PAGE, followed by transfer to PVDF membranes (ISEQ00010; Millipore, Burlington, USA). The membranes were blocked with 5% bovine serum albumin (A7906; Sigma-Aldrich) and subsequently probed with the indicated primary antibodies, including mouse anti-β-actin (66009-1-Ig, 1:5000; Proteintech, Wuhan, China), mouse anti-GAPDH (60004-1-Ig, 1:5000; Proteintech), rabbit anti-EZH2 (21800-1-AP, 1:1000; Proteintech), rabbit anti-H3K27me3 (ab192985, 1:1000; Abcam, Cambridge, UK), rabbit anti-BCL-2 (12789-1-AP, 1:5000; Proteintech), rabbit anti-γH2AX (10856-1-AP, 1:1000; Proteintech), rabbit anti-Cyclin D1 (26939-1-AP, 1:1000; Proteintech) and rabbit anti-STAT3 (10253-2-AP, 1:1000; Proteintech), rabbit anti-p65 (10745-1-AP, 1:1000; Proteintech), rabbit anti-β-catenin (51067-2-AP, 1:1000; Proteintech), rabbit anti-AKT (10176-2-AP, 1:1000; Proteintech), and rabbit anti-RAP1 (RAP1A + RAP1B) (ab187659, 1:1000; Abcam), followed by fluorescently labeled secondary antibodies anti-mouse or anti-rabbit, both from Li-Cor (926-32211, 926-32210; Lincoln, USA). Protein signals were detected using a fluorescence imaging system (Odyssey; Li-Cor). For proteasome inhibition experiments, cells were treated with MG132 (HY-13259; MedChemExpress, Monmouth Junction, USA) before protein extraction and

western blot analysis.

siRNA-mediated knockdown of *EZH2* and *STAT3*

Small interfering RNAs (siRNAs) targeting *EZH2* and *STAT3*, along with a non-targeting control siRNA (siNC), were purchased from a commercial supplier (GenePharma, Shanghai, China). The sequences were as follows: *EZH2* siRNA#1, sense 5′-GGAGUUGGU GAAUGCCCUUTT-3′ and antisense 5′-AAGGGCAUUCACCAA CUCCTT-3′; *EZH2* siRNA#2, sense 5′-GCUCCUCUAACCAU GUUUATT-3′ and antisense 5′-UAAACAUGGUUAGAGGAGCTT-3′; *STAT3* siRNA#1, sense 5′-AGAGUCGAAUGUUCUCUAU-3′ and antisense 5′-AUAGAGAACAUUCGACUCU-3′; *STAT3* siRNA#2, sense 5′-GCUUCCUGCAAGAGUCGAA-3′ and antisense 5′-UUCGA CUCUUGCAGGAAGC-3′; negative control siRNA (siNC), sense 5′-UUCUCCGAACGUGUCACGUTT-3′ and antisense 5′-ACGUGACAC GUUCGGAGAATT-3′. Cells were seeded in 6-well plates and transfected with siRNAs using Lipofectamine 3000 transfection reagent (L3000150; Invitrogen, Carlsbad, USA) according to the manufacturer's instructions. Briefly, siRNAs were diluted in Opti-MEM (31985070; Gibco) and incubated with the transfection reagent to form complexes, which were then added to the cells at a final concentration of 50 nM. A non-targeting siRNA control was included in all experiments to exclude potential off-target effects. After 48 h of transfection, cells were harvested for subsequent analyses, including quantitative PCR and western blotting to confirm knockdown efficiency. All experiments were performed in at least three independent replicates.

Lentiviral overexpression of EZH2

For stable overexpression of EZH2, the full-length human EZH2 coding sequence was cloned into a lentiviral expression vector, pLVX (632164; Clontech Laboratories, Mountain View, USA). Lentiviral particles were produced by co-transfecting HEK293T cells (ATCC) with the EZH2 expression vector and packaging plasmids, psPAX2 and pMD2.G (Addgene, Watertown, USA), using Lipofectamine™ 3000 Transfection Reagent (L3000150; Invitrogen). Viral supernatants were collected at 48 and 72 h post-transfection, filtered, and used to infect target cells in the presence of polybrene (H9268; Sigma-Aldrich) at a final concentration of 8 μg/mL. After 48 h of infection, cells were selected with puromycin (P8833; Sigma-Aldrich) at 2 μg/mL to establish stable cell lines. Overexpression efficiency was verified by quantitative PCR and western blot analysis. Quantitative PCR was performed using ChamQ SYBR qPCR Master Mix (Q311-02; Vazyme, Nanjing, China) on a QuantStudio 5 Real-Time PCR System (Applied Biosystems, Foster City, USA). The primer sequences used for qPCR were as follows: *EZH2* forward, 5′-TACAGTGGAGGATGCCCTGA-3′, and reverse, 5′-TGCTGGCATAGATTACCCGC-3′; *STAT3* forward, 5′-CAGCAGCTT GACACACGGTA-3′, and reverse, 5′-AAACACCAAAGTGGCATGT GA-3′; *GAPDH* forward, 5′-GGAGCGAGATCCCTCCAAAAT-3′, and reverse, 5′-GGCTGTTGTCATACTTCTCATGG-3′. *GAPDH* was used as the internal control for normalization.

Apoptosis and cell cycle analysis

Apoptosis was assessed using the Annexin V-PE/7-AAD detection kit (40310ES20; Yeasen, Shanghai, China) according to the manufacturer's instructions. Briefly, cells were treated with pomalidomide at the IC_{50} concentration of each parental cell line for 48 h, then harvested, washed twice with cold PBS, and resuspended in 1× binding buffer. Cells were subsequently incubated with Annexin V-PE and 7-AAD in the dark at room temperature for 15 min. After staining, samples were immediately analyzed using a flow cytometer (BD FACSCanto II; BD Biosciences, San Jose, USA), and data were processed with FlowJo software (Version 10.8.1; BD Life Sciences, Ashland, USA) to quantify the percentages of early and late apoptotic cells.

For cell cycle analysis, cells were collected, washed with PBS, and fixed in 70% ethanol at 4°C overnight. Fixed cells were then washed and incubated with propidium iodide (556463; BD Biosciences) staining solution containing RNase A (R4875; Sigma-Aldrich) at 37°C for 30 min in the dark. DNA content was measured by flow cytometry, and cell cycle distribution was analyzed using FlowJo software.

Cycloheximide (CHX) chase assay

To evaluate STAT3 protein stability, pomalidomide-resistant MM cells transfected with control or EZH2-targeting siRNAs were treated with cycloheximide (C7698; Sigma-Aldrich) to inhibit *de novo* protein synthesis. At the indicated time points after CHX exposure, cells were harvested and lysed, and STAT3 protein levels were examined by western blot analysis. Protein band intensities were quantified using ImageJ software (Version 1.54; National Institutes of Health, Bethesda, USA). Relative protein expression levels were normalized to the corresponding loading controls and expressed relative to the control group. The relative abundance of STAT3 at each time point was expressed as a fraction of the initial level to estimate protein degradation kinetics.

Immunoprecipitation and ubiquitination assay

Cells were lysed in ice-cold NP-40 lysis buffer (P0013F; Beyotime Biotechnology) supplemented with protease inhibitors (P1005; Beyotime Biotechnology) and 10 mM N-ethylmaleimide (E3876; Sigma-Aldrich) to preserve ubiquitin conjugates. Equal amounts of protein were incubated with anti-STAT3 antibody overnight at 4°C with gentle rotation, followed by incubation with protein A/G agarose beads (P2012; Beyotime Biotechnology) for 2–4 h. Immunocomplexes were washed extensively with lysis buffer and eluted by boiling in SDS sample buffer. Eluted proteins were resolved by 8% SDS-PAGE and analyzed by western blot analysis using an anti-ubiquitin antibody to assess STAT3 ubiquitination. Total STAT3 levels in the immunoprecipitates were evaluated to confirm comparable immunoprecipitation efficiency across samples.

Co-immunoprecipitation (Co-IP)

Cells were lysed in Co-IP lysis buffer (50 mM Tris-HCl, pH 7.4, 150 mM NaCl, 1% NP-40, 10% glycerol, and protease inhibitors) and incubated on ice for 30 min. The lysates were then centrifuged at 12,000 *g* for 15 min at 4°C to remove cellular debris. The supernatant was pre-cleared by incubating with 30 μL of protein A/G agarose beads for 1 h at 4°C. For immunoprecipitation, 1–2 μg of the specific primary antibody was added to the pre-cleared lysate and incubated overnight at 4°C with rotation. Afterward, protein A/G agarose beads (30 μL) were added to the mixture and incubated for 2 h at 4°C. The beads were washed three times with washing buffer (50 mM Tris-HCl, pH 7.4, 150 mM NaCl, and 0.1% NP-40) and resuspended in loading buffer. Proteins were separated by 10% SDS-PAGE, transferred to PVDF membranes, and detected by

western blot analysis using the appropriate antibodies

RNA sequencing (RNA-seq)

Total RNA was extracted from multiple myeloma cells, either untreated or subjected to drug exposure, using TRIzol reagent (Invitrogen). The integrity and concentration of the isolated RNA were determined with an Agilent 2100 Bioanalyzer (Agilent Technologies, Santa Clara, USA). Sequencing libraries were subsequently prepared using the Illumina TruSeq RNA kit (RS-122-2001; Illumina, San Diego, USA) and subjected to paired-end 150 bp sequencing on the HiSeq 4000 platform (Illumina).

Differential gene expression analysis

DESeq2 Differential expression analysis was performed using the DESeq2 R package (Bioconductor) with a $|\log2 \text{ Fold Change}| > 1$ and a P value < 0.05 as the selection criteria. Gene Ontology (GO) and Kyoto Encyclopedia of Genes and Genomes (KEGG) pathway analyses were conducted using the ClusterProfiler package in R software (Version 4.3.1) originally developed by Ross Ihaka and Robert Gentleman (https://www.r-project.org/).

Gene set enrichment analysis (GSEA)

GSEA was performed using GSEA software v4.3.2 developed by the Broad Institute (https://www.gsea-msigdb.org/gsea/index.jsp). All gene sets were selected, and pathways were enriched in drug-resistant cells post-si-*EZH2* treatment. Results were visualized using bubble plots and heatmaps to illustrate activated or suppressed pathways.

Xenograft mouse models

All procedures involving mice were approved by the local ethical committee for animal experimentation. Female NCG (NOD/ShiLtJGpt-Prkdcem26Cd52Il2rgem26Cd22/Gpt) mice, aged 4 weeks, were purchased from GemPharmatech (Suzhou, China) and allowed to acclimatize for 1 week prior to tumor cell inoculation. At 5 weeks of age, NCG mice were injected subcutaneously into the right flank with 5×10^6 U266 PR cells. Once the tumor volume reached 140 to 200 mm^3, the mice were randomly assigned to one of the four treatment groups ($n = 5$ per group): vehicle control, pomalidomide monotherapy, GSK343 monotherapy, and pomalidomide plus GSK343 combination treatment. Animals were randomly assigned to experimental groups using a computer-generated randomization algorithm. Prior to treatment, each animal was individually numbered and assigned to either the treatment or control group, ensuring a balanced distribution based on baseline characteristics such as body weight and health status. Randomization was performed by a blinded investigator to minimize bias. All animals were housed under standard laboratory conditions and monitored regularly throughout the study. Pomalidomide was administered by oral gavage at a dose of 5 mg/kg daily in the monotherapy group, while GSK343 was given by intraperitoneal injection at 5 mg/kg every other day. In the combination group, pomalidomide was administered at 3 mg/kg by oral gavage, and GSK343 at 2 mg/kg by intraperitoneal injection every other day. Tumor growth and body weight were measured every 3 days, and tumor volume was calculated using the formula: $0.5 \times \text{length (mm)} \times \text{width}^2 \text{ (mm)}$ with a caliper. At the study endpoint, mice were deeply anesthetized with isoflurane and subsequently sacrificed by cervical dislocation to ensure death, in accordance with institutional animal care and ethical guidelines. All animal experiments were approved by the Ethics Committee of Soochow University (approval No. 202504A0940). The study was conducted in accordance with the Declaration of Helsinki.

Histological analysis

Tissues were fixed in 10% formalin (Sigma-Aldrich), embedded in paraffin, and sectioned. Hematoxylin and eosin (H & E) staining was performed to assess tissue morphology and potential toxicity. Tumor and major organ tissues were fixed in 4% paraformaldehyde, embedded in paraffin, sectioned at 4 μm, and subjected to routine H & E staining. Histopathological changes were examined under a light microscope (Olympus, Tokyo, Japan).

Statistical analysis

All statistical analyses were performed using GraphPad Prism software (Version 9.0). For comparisons between two groups, a two-tailed unpaired Student's t test was used. Data are expressed as the mean ± standard deviation (SD), and a P value of < 0.05 was considered statistically significant.

Results

EZH2 is highly expressed in MM and associated with a poor prognosis

To assess EZH2 expression in multiple myeloma and its association with patient outcomes, we interrogated the GSE6477 cohort comprising newly diagnosed MM (NDMM) and RRMM cases. This analysis revealed a marked increase in EZH2 transcript abundance in RRMM samples compared with NDMM samples. To explore any associations between EZH2 and clinical outcomes in RRMM patients, we analyzed data from the GSE2658 dataset and found that higher *EZH2* mRNA levels were associated with poorer overall survival (Figure 1A). These results demonstrate that upregulation of EZH2 in RRMM correlates with a poor prognosis.

EZH2 is upregulated in pomalidomide-resistant MM cells

To investigate the molecular mechanisms driving pomalidomide resistance in MM, we established two pomalidomide-resistant cell lines, MM.1S PR and U266 PR, through repeated high-dose pulse selection (Figure 1B). Drug sensitivity assays revealed a marked increase in IC_{50} for pomalidomide in the resistant cells compared to parental cells, indicating successful induction of resistance (Figure 1B). Consistently, flow cytometry-based apoptosis assays showed significantly reduced pomalidomide-induced apoptosis in resistant cells, further confirming the resistant phenotype (Figure 1C). Finally, in proliferation assays, the resistant cell lines exhibited enhanced proliferative capacity under normal culture conditions, suggesting that the acquisition of drug resistance may be accompanied by increased cell fitness (Figure 1D).

To explore the molecular changes associated with resistance, we assessed the expression of EZH2 and its downstream histone modification H3K27me3. Quantitative polymerase chain reaction (qPCR) and western blot analysis revealed significant upregulation of EZH2 at both the mRNA and protein levels in resistant cells (Figure 1E,F). In parallel, H3K27me3 levels were markedly elevated in pomalidomide-resistant cells and showed a pattern consistent with EZH2 expression, suggesting that EZH2-mediated epigenetic regulation may be involved in the development of pomalidomide

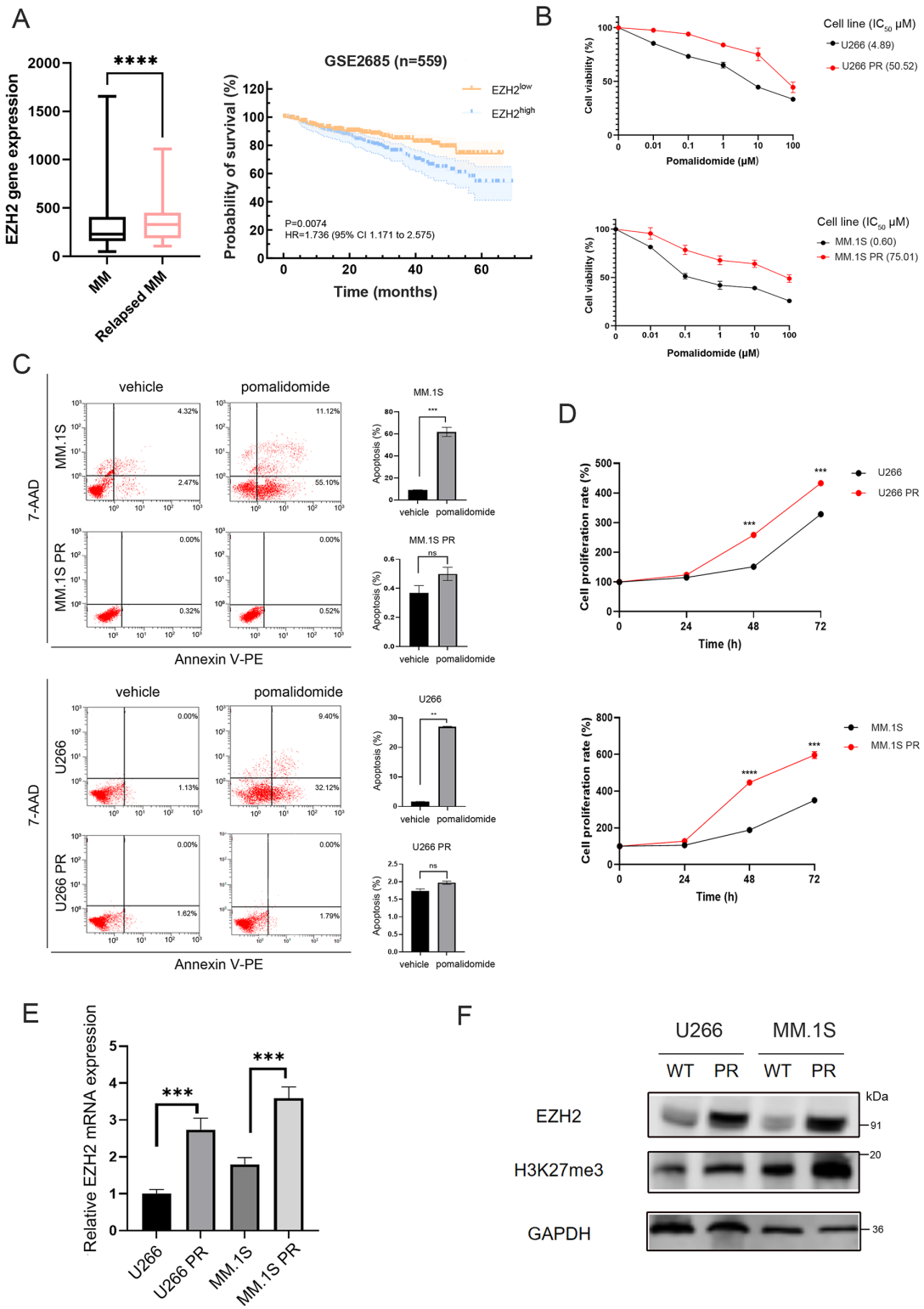


Figure 1. EZH2 is upregulated in RRMM and in pomalidomide-resistant cell lines (A) Analysis of EZH2 expression in NDMM and relapsed/refractory MM (RRMM) cases in the GSE6477 dataset. EZH2 expression was higher in RRMM than in NDMM, and among cases in the GSE2658 dataset, higher EZH2 levels were associated with poorer overall survival. (B) IC_{50} values for pomalidomide in parental and resistant MM.1S and U266 cell lines were determined by CCK-8 assay and confirmed the successful establishment of pomalidomide-resistant models. (C) Flow cytometry-based apoptosis analysis demonstrated reduced pomalidomide-induced apoptosis in resistant cells. (D) Proliferation assays showed enhanced growth of resistant cell lines under normal culture conditions. (E,F) qPCR and western blot analyses showed upregulation of *EZH2* mRNA and protein in resistant cells, accompanied by increased H3K27me3 levels. Data are presented as the mean ± SD. $^{**}P < 0.01$, $^{***}P < 0.001$; ns, not significant.

resistance (Figure 1F).

EZH2 is a central regulator of distinct resistance mechanisms in pomalidomide-resistant MM cells

To further elucidate the molecular mechanisms underlying pomalidomide resistance and the role of EZH2, we performed high-throughput RNA sequencing on paired parental and pomalidomide-resistant MM cell lines. Differential gene expression analysis revealed significant transcriptional reprogramming in both resistant cell lines compared to their parental counterparts (Figure 2A). Volcano plot visualization revealed highly elevated EZH2 expression in resistant cells, indicating a potential association with the resistant phenotype (Figure 2B). GSEA further demonstrated consistent enrichment of H3K27me3-associated gene repression signatures in both resistant cell models, suggesting an epigenetic regulatory shift driven by EZH2 (Figure 2C).

To explore the functional implications of these transcriptional changes, we performed GO and KEGG pathway enrichment analyses on the identified differentially expressed genes. The results revealed two major categories of resistance-associated pathways: (1) nuclear mechanisms involving DNA repair, chromatin remodeling, and epigenetic regulation and (2) cytoplasmic mechanisms characterized by cytoskeletal remodeling, cell polarity, migration, and metabolic adaptation (Figure 2D,E). Interestingly, EZH2 emerged as a key upstream node integrating the two resistance mechanisms. It was found to transcriptionally regulate nuclear factors such as RAD51 and BRCA1, which are involved in homologous recombination, as well as cytoplasmic effectors, including cell division cycle 42 (CDC42), hypoxia-inducible factor 1 alpha (HIF1A), and vascular endothelial growth factor A (VEGFA), which are associated with cytoskeletal dynamics and metabolic plasticity.

These findings suggest that EZH2 may drive pomalidomide resistance by orchestrating a genome-wide transcriptional program through H3K27me3-mediated repression, with effects on both nuclear and cytoplasmic adaptive systems. The central role of EZH2 in coordinating diverse resistance pathways highlights its therapeutic potential as a master regulator and target in RRMM.

EZH2 inhibition reverses pomalidomide resistance and has synergistic anti-myeloma effects

Given the functional involvement of EZH2 in pomalidomide resistance, we hypothesized that pharmacological inhibition of EZH2 could restore the drug sensitivity of MM cells. To test this hypothesis, we screened two classes of EZH2-targeting compounds: enzymatic inhibitors and proteolysis targeting chimera (PROTAC)-based degraders. EZH2 inhibitors, such as GSK343, suppress methyltransferase activity and disrupt polycomb repressive complex 2 (PRC2) integrity, whereas PROTAC degraders (*e.g.*, MS1943) induce EZH2 degradation via the ubiquitin-proteasome pathway. Drug sensitivity assays revealed that GSK343 exerted cytotoxic effects on both parental and pomalidomide-resistant MM cells, with notably greater efficacy in resistant cells. In contrast, the EZH2 PROTAC degrader MS1943 displayed minimal activity in parental cells but effectively suppressed the viability of resistant cells (Figure 3A, left). We treated the cells with MS1943, and the western blot analysis results indicated that MS1943 effectively reduced the expression level of EZH2 (Figure 3A, right). This differential response suggests that EZH2 contributes to pomalidomide resistance not only through its canonical methyltransferase activity but also via non-catalytic mechanisms, such as structural or protein-protein interaction-mediated functions.

We next evaluated the combinatorial effects of GSK343 and pomalidomide. Co-treatment assays demonstrated a synergistic inhibition of cell proliferation in resistant cells (Figure 3B). To further evaluate the therapeutic potential of EZH2 targeting *in vivo*, we selected GSK343 for subsequent animal studies based on its well-characterized pharmacokinetic profile, molecular stability, and *in vitro* potency. *In vivo*, resistant MM xenografts in NCG mice were treated with vehicle, pomalidomide, GSK343, and the combination of both pomalidomide and GSK343 for 15 days. Tumor volumes were similar between the vehicle and pomalidomide monotherapy groups, confirming the resistant phenotype (Figure 3C, left). GSK343 monotherapy significantly reduced the tumor burden, while the combination treatment caused marked tumor regression, demonstrating a strong synergistic effect (Figure 3C, left). This combination strategy could allow dose reduction of pomalidomide while maintaining efficacy, suggesting translational potential for overcoming resistance with reduced toxicity. Throughout the duration of treatment, the mice showed no significant changes in body weight, indicating that GSK343 was well tolerated and did not elicit overt systemic toxicity (Figure 3C, right). To further confirm the compound's safety profile, comprehensive histopathological examinations of major organs, including the liver, kidney, heart, and lung, were conducted post-treatment. These analyses revealed no discernible tissue damage or pathological abnormalities, supporting the conclusion that GSK343 administration does not induce organ-specific toxicity at the therapeutic doses used (Figure 3D).

Flow cytometry-based apoptosis analysis further confirmed that treatment with GSK343 not only reversed pomalidomide resistance but also enhanced apoptosis among MM cells when administered in combination with pomalidomide (Figure 3E).

Importantly, we also extended our findings to primary patient-derived MM cells. *In vitro* drug sensitivity testing on $CD138^+$ cells from NDMM and RRMM patients showed that GSK343 had broad anti-myeloma activity. Notably, GSK343 was particularly effective in RRMM samples, where it not only suppressed cell viability but also partially restored sensitivity to pomalidomide (Figure 3F). These results further support the translational relevance of EZH2 as a therapeutic target for overcoming drug resistance in MM.

EZH2 bidirectionally regulates pomalidomide sensitivity, with *EZH2* knockdown inducing apoptosis and cell cycle arrest in pomalidomide-resistant MM cells

To further investigate the functional role of EZH2 in pomalidomide resistance, we performed *EZH2* knockdown in resistant MM cell lines using two independent small interfering RNAs (siRNAs). Knockdown efficiency was confirmed at both the mRNA and protein levels by qPCR and western blot analysis, respectively (Figure 4A). Drug sensitivity assays revealed that silencing of *EZH2* partially restored the sensitivity of resistant cells to pomalidomide, indicating that EZH2 contributes to the maintenance of the resistant phenotype (Figure 4B). We next assessed the effect of *EZH2* knockdown on cell proliferation. Compared with the negative control, both si-*EZH2*-treated groups exhibited reduced proliferation, with growth inhibition becoming evident at 48 h post transfection. These results suggest that EZH2 not only promotes

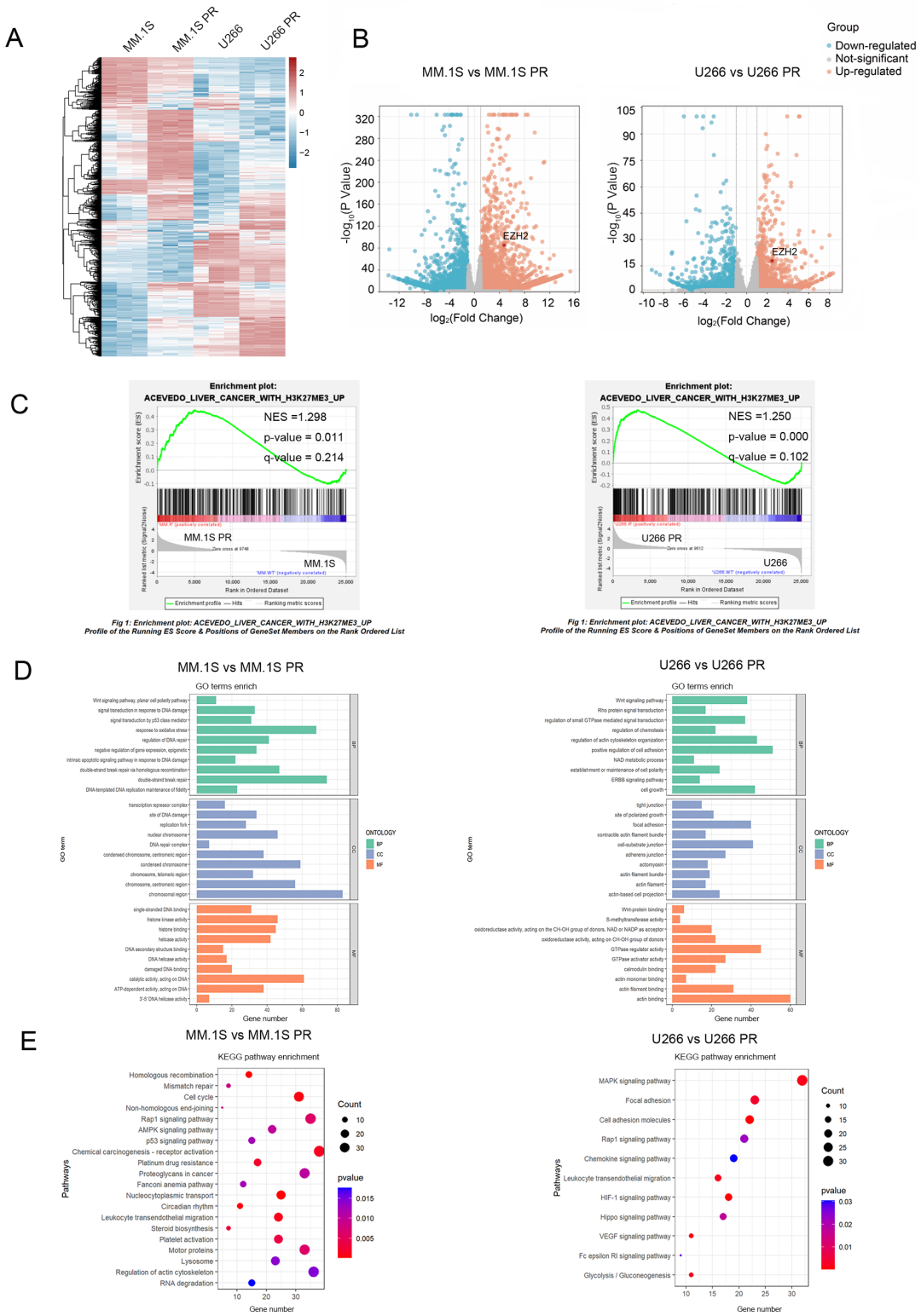


Figure 2. Transcriptomic profiling identifies EZH2 as a central regulator of distinct resistance mechanisms in pomalidomide-resistant MM cells
(A) Heatmap of differentially expressed genes between parental and resistant MM cell lines. (B) Volcano plot showing elevated EZH2 expression in resistant cells. (C) GSEA indicating enrichment of H3K27me3-associated gene repression signatures in resistant cells. (D,E) Gene Ontology (GO) and KEGG pathway enrichment analyses of differentially expressed genes revealed two major categories of resistance mechanisms: nuclear pathways (DNA repair, chromatin remodeling, and epigenetic regulation) and cytoplasmic pathways (cytoskeletal remodeling, cell polarity, migration, and metabolic adaptation). EZH2 was identified as a key upstream node integrating both resistance mechanisms via the regulation of both nuclear effectors (*e.g.*, RAD51, BRCA1) and cytoplasmic effectors (*e.g.*, CDC42, HIF1A, VEGFA).

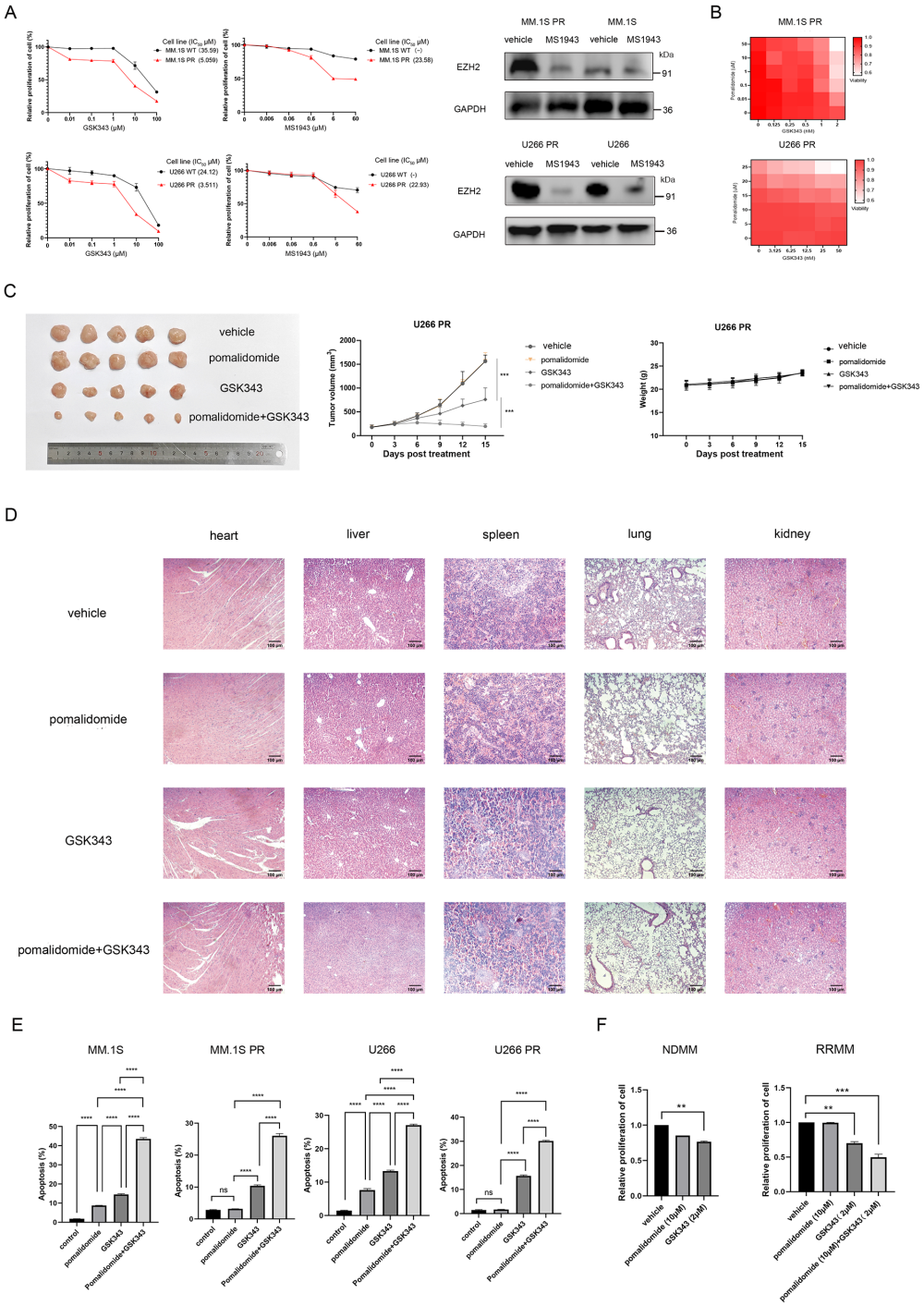


Figure 3. Pharmacological inhibition of EZH2 reverses pomalidomide resistance and exerts synergistic anti-myeloma effects both *in vitro* and *in vivo* (A) Drug sensitivity assays showed the cytotoxic effects of the EZH2 inhibitor GSK343 and PROTAC degrader MS1943 on parental and pomalidomide-resistant MM cells. GSK343 exhibited greater efficacy in resistant cells, while MS1943 was minimally active in parental cells but suppressed resistant cell viability. Western blot analysis results indicated that MS1943 effectively reduced the expression level of EZH2. (B) Co-treatment with GSK343 and pomalidomide led to synergistic inhibition of cell proliferation in resistant MM. (C) *In vivo* murine xenograft model using resistant MM cells treated with vehicle, pomalidomide, GSK343, or the combination for 2 weeks. Tumor volumes and body weights are shown. GSK343 monotherapy significantly reduced the tumor burden, and the combination therapy induced marked tumor regression without overt toxicity. (D) Representative H&E staining images of major organs (heart, liver, spleen, lung, and kidney) from mice at the end of treatment. No signs of significant tissue damage or toxicity were observed. (E) Flow cytometry-based apoptosis analysis demonstrated enhanced apoptosis in resistant cells treated with GSK343, either alone or in combination with pomalidomide. (F) Drug sensitivity of $CD138^+$ primary MM cells from NDMM and RRMM patients. GSK343 suppressed cell viability in both NDMM and RRMM samples and partially restored sensitivity to pomalidomide in RRMM cells. Data are presented as the mean ± SD. $^{**}P < 0.01$, $^{***}P < 0.001$, $^{****}P < 0.0001$; ns, not significant.

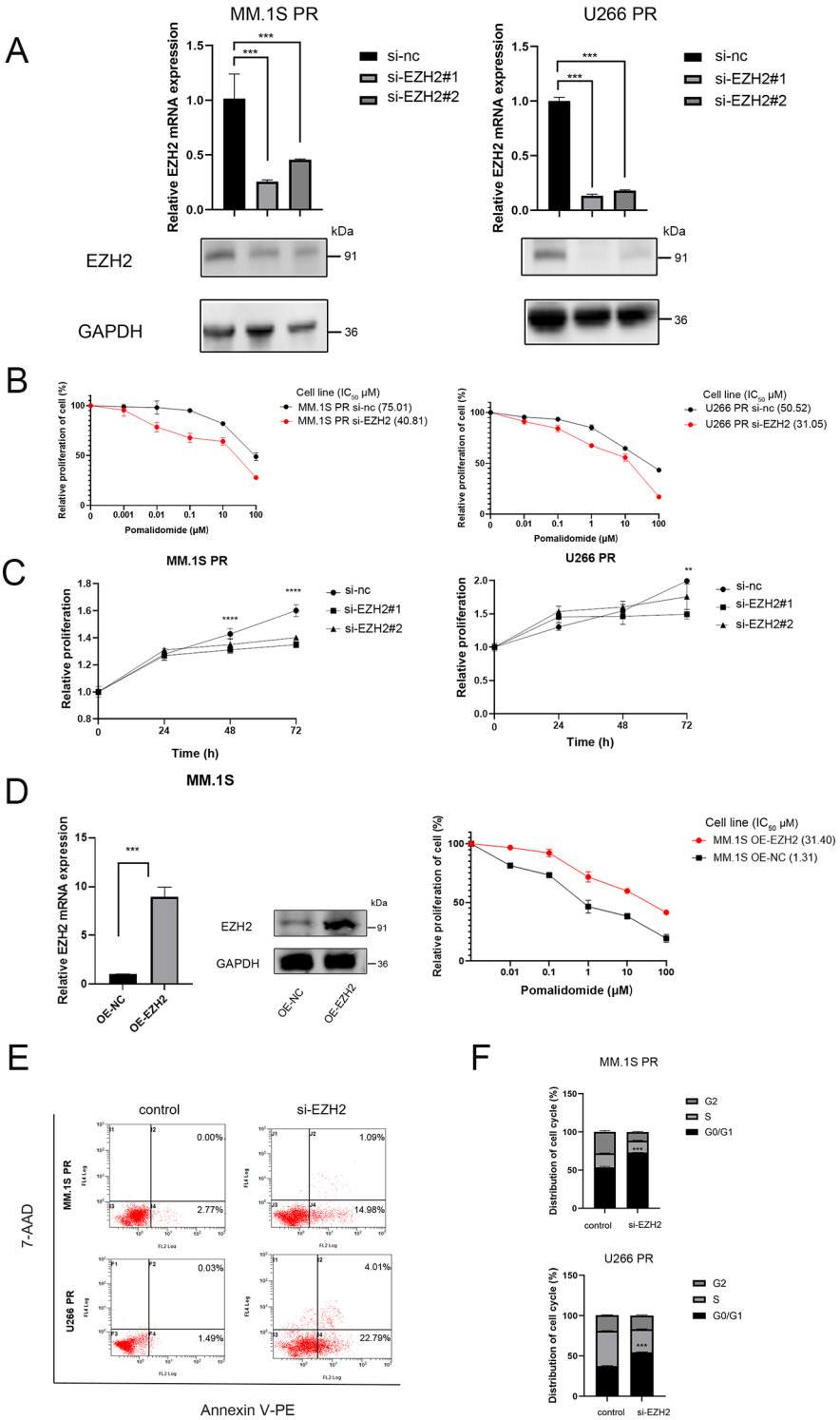


Figure 4. EZH2 bidirectionally regulates pomalidomide sensitivity, while *EZH2* knockdown enhances apoptosis and induces G1-phase cell cycle arrest in resistant MM cells (A) Treatment with two independent siRNAs resulted in *EZH2* knockdown in resistant MM cell lines at both the mRNA and protein levels, as determined by qPCR and western blot analysis. (B) Drug sensitivity assays showed partial restoration of pomalidomide sensitivity in resistant cells after *EZH2* knockdown. (C) Proliferation assays demonstrated reduced cell growth after *EZH2* silencing, with growth inhibition evident at 48 h post-transfection. (D) Overexpression of EZH2 in MM cell lines was confirmed at both the mRNA and protein levels by qPCR and western blot analysis. Forced expression of EZH2 in parental MM cell lines reduced sensitivity to pomalidomide, as assessed by cell viability assays following drug treatment. (E) Flow cytometric analysis showed increased apoptosis in resistant cells upon *EZH2* knockdown compared with the control. (F) Cell cycle analysis revealed G1-phase arrest in resistant MM cells after *EZH2* knockdown, indicating that inhibition of EZH2 suppresses proliferation by disrupting normal cell cycle progression. Data are presented as the mean ± SD, $^{**}P < 0.01$, $^{***}P < 0.001$, $^{****}P < 0.0001$.

drug resistance but also enhances proliferative capacity in resistant MM cells (Figure 4C). To further establish causality, we performed EZH2 gain-of-function experiments in parental, pomalidomide-sensitive MM cells. Overexpression of EZH2 significantly decreased pomalidomide sensitivity, indicating that elevated EZH2 expression is sufficient to promote a resistant phenotype (Figure 4D).

To further explore the impact of EZH2 on pomalidomide resistance, we first assessed apoptosis in pomalidomide-resistant MM cells following *EZH2* knockdown. Flow cytometric analysis revealed a marked increase in apoptotic cell numbers following *EZH2* knockdown compared with control groups, indicating that EZH2 depletion enhances apoptosis in resistant cells (Figure 4E). We next performed cell cycle analysis to evaluate the impact of *EZH2* knockdown on cell proliferation. *EZH2* knockdown induced significant accumulation of cells in the G1 phase in both resistant cell models compared with vehicle controls, suggesting that EZH2 inhibition suppresses proliferation by causing G1 phase arrest and disrupting normal cell cycle progression (Figure 4F).

EZH2 maintains pomalidomide resistance by stabilizing STAT3 to regulate apoptosis and the cell cycle and may additionally contribute to DNA repair processes

To elucidate how EZH2 contributes to pomalidomide resistance, we performed high-throughput RNA sequencing of resistant MM cells after *EZH2* knockdown. GSEA revealed substantial alterations across multiple biological processes, with significant enrichment in pathways regulating cell cycle progression, apoptosis, and DNA repair (Figure 5A). These findings indicate that the resistant phenotype is supported by multiple coordinated survival programs and that disruption of EZH2 perturbs all three axes simultaneously.

KEGG and GO enrichment analyses further reinforced these observations. In addition to pathways associated with histone methylation and chromatin modification, which reflect canonical EZH2 catalytic activity, these analyses identified a broader array of enriched pathways involving cell cycle control, apoptosis regulation, and DNA damage repair (Figure 5B,C). Many of these pathways are not exclusively linked to the methyltransferase function of EZH2, suggesting that EZH2 may contribute to the maintenance of pomalidomide resistance through both enzymatic and non-enzymatic roles. These findings provide a rationale for examining downstream nodes beyond classical PRC2 targets.

Among the enriched pathways, JAK-STAT signaling consistently appeared with relatively high enrichment scores across cell models (Figure 5B). Because STAT3 is a central regulator of survival signaling, apoptosis suppression, and G1-S transition and because its downstream functions overlap with processes disrupted by *EZH2* knockdown, STAT3 emerged as a biologically coherent candidate linking EZH2 activity with the pomalidomide-resistant MM cell phenotype. We therefore investigated whether EZH2 regulates STAT3 in resistant cells. Western blot analysis showed that *EZH2* knockdown resulted in a marked decrease in STAT3 protein abundance, whereas qPCR showed no change in STAT3 mRNA expression (Figure 6A,B). This dissociation indicates a post-transcriptional regulatory mechanism. To determine whether this effect was specific to STAT3, we further evaluated several unrelated signaling molecules, including NF-κB, β-catenin, Akt, and Rap1. No significant alterations were observed following EZH2 modulation (Supplementary Figure S1B), supporting the specificity of the EZH2-STAT3 regulatory axis. Correspondingly, *EZH2* knockdown led to reduced expression of downstream survival and cell cycle regulators, including B-cell lymphoma-2 (Bcl-2) and Cyclin D1, accompanied by an increase in γH2AX expression, indicating enhanced DNA damage (Figure 6A). To determine whether the reduction in the STAT3 protein level results from enhanced proteasomal turnover, resistant cells were treated with the proteasome inhibitor MG132 after *EZH2* knockdown. MG132 partially restored the STAT3 protein level, indicating that EZH2 maintains STAT3 abundance by preventing proteasome-mediated degradation (Figure 6C). To further assess whether *EZH2* knockdown accelerates STAT3 protein turnover, we performed cycloheximide (CHX) chase assays to monitor STAT3 stability over time. STAT3 protein levels declined more rapidly in si-*EZH2*-treated resistant cells than in siNC controls following CHX treatment, indicating a shortened STAT3 protein half-life upon EZH2 depletion (Figure 6D). Consistent with the accelerated STAT3 degradation observed in the CHX chase assay, we further examined whether EZH2 depletion affects STAT3 ubiquitination. To this end, STAT3 was immunoprecipitated from pomalidomide-resistant MM cells transfected with control or *EZH2*-targeting siRNA, followed by western blot analysis for ubiquitin. *EZH2* knockdown resulted in increased ubiquitination of STAT3 compared with that in control cells, while comparable levels of total STAT3 were recovered in the immunoprecipitates (Supplementary Figure S1C). These findings indicate that loss of EZH2 promotes STAT3 ubiquitination, providing additional evidence that EZH2 contributes to STAT3 protein stabilization by limiting its proteasome-targeting modification. To further investigate whether the regulation of STAT3 by EZH2 depends on direct protein-protein interactions, we performed Co-IP assay in pomalidomide-resistant MM cells. The results demonstrated that STAT3 was specifically co-precipitated with the EZH2 antibody, and this interaction was consistently observed in both resistant cell lines. These findings suggest that EZH2 forms a complex with STAT3 within cells, indicating that EZH2 may regulate the stability of STAT3 through direct binding (Figure 6E). Together, these results suggest that EZH2 contributes to the stabilization of the STAT3 protein by interacting with it, thereby preventing proteasome-mediated degradation and maintaining STAT3 stability in pomalidomide-resistant MM cells.

To define the functional consequences of STAT3 suppression, we validated effective *STAT3* knockdown at both the mRNA and protein levels in resistant cells (Figure 6F). *STAT3* silencing resulted in the restoration of key features of the si-*EZH2*-induced phenotype, including the downregulation of Bcl-2 and Cyclin D1 (Figure 6G), supporting the STAT3-Bcl-2/Cyclin D1 axis as a major downstream effector through which EZH2 promotes survival and proliferation. However, *STAT3* knockdown did not reproduce the full increase in γH2AX observed in si-*EZH2*-treated cells, indicating that EZH2 may modulate DNA repair through additional STAT3-independent pathways.

To independently test whether pharmacologic EZH2 inhibition affects STAT3 stability, we examined resistant cells treated with the EZH2 inhibitor GSK343. GSK343 treatment induced reductions in STAT3 protein and corresponding downstream markers (p65, β-catenin, Akt, and Rap1; Figure 6H), mirroring the effects of *EZH2* knockdown. These results demonstrate that EZH2 enzymatic inhibition alone is sufficient to destabilize STAT3, suggesting that the catalytic activity of EZH2 contributes to STAT3 maintenance, although non-catalytic mechanisms cannot be excluded.

Together, these findings support a mechanistic model in which

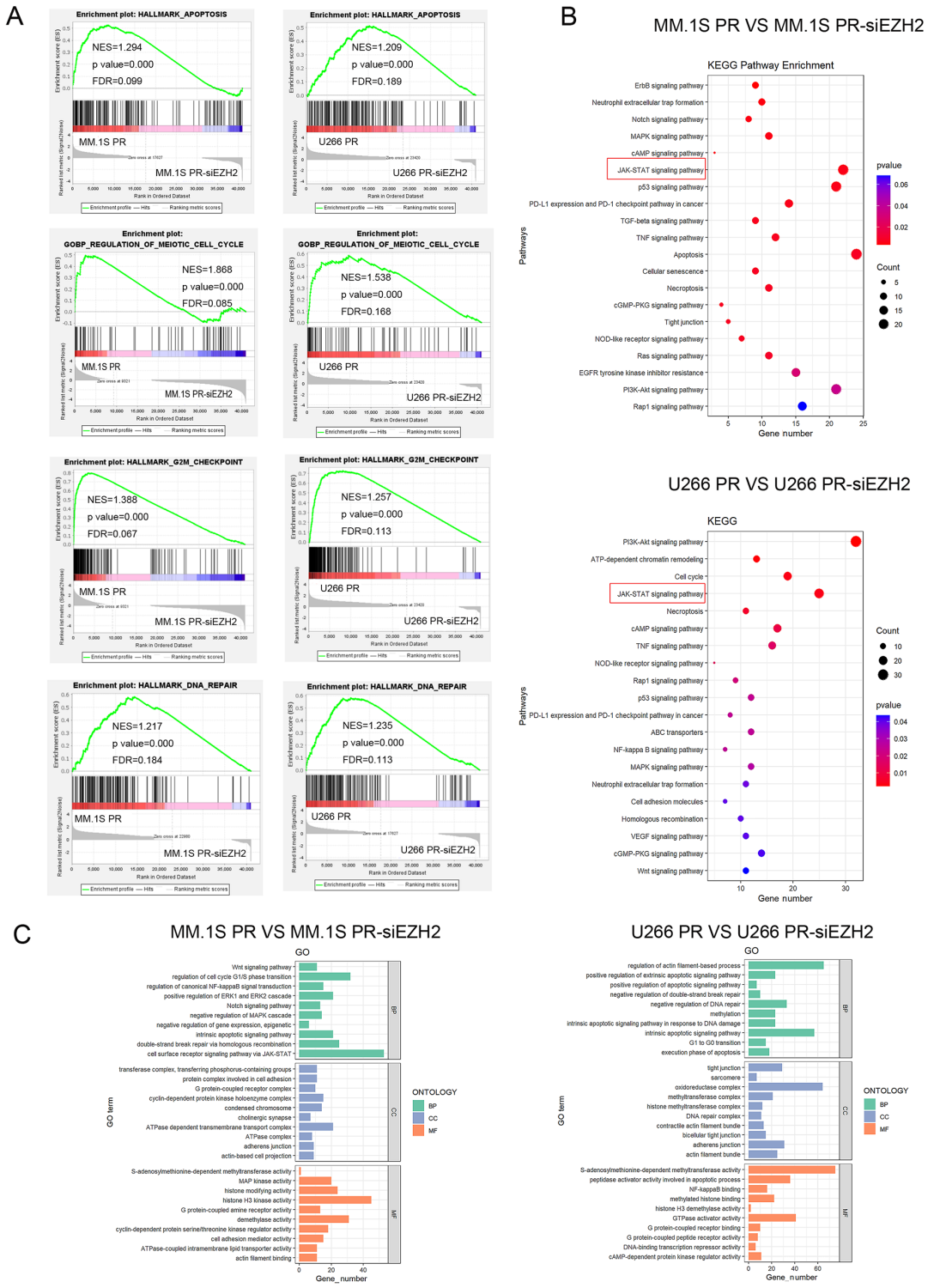


Figure 5. Transcriptomic analysis reveals that EZH2 regulates the cell cycle, apoptosis, and DNA repair pathways in pomalidomide-resistant MM cells (A) GSEA showed significant enrichment of cell cycle, apoptosis, and DNA repair pathways in resistant MM cells upon *EZH2* knockdown (si-*EZH2*). (B) KEGG pathway enrichment analysis of differentially expressed genes in si-*EZH2*-treated resistant cells highlighted histone methylation-related pathways as well as high-ranking enrichment of the JAK-STAT signaling pathway in both MM.1S PR and U266 PR cells. (C) GO enrichment analysis of differentially expressed genes in si-*EZH2*-treated resistant cells. Histone methylation-related pathways were significantly enriched, supporting the canonical methyltransferase-dependent functions of EZH2. In contrast, the results also showed enrichment of many pathways associated with cell cycle regulation and apoptosis, indicating that EZH2 may also contribute to drug resistance through noncanonical, methyltransferase-independent mechanisms that affect cell proliferation and survival.

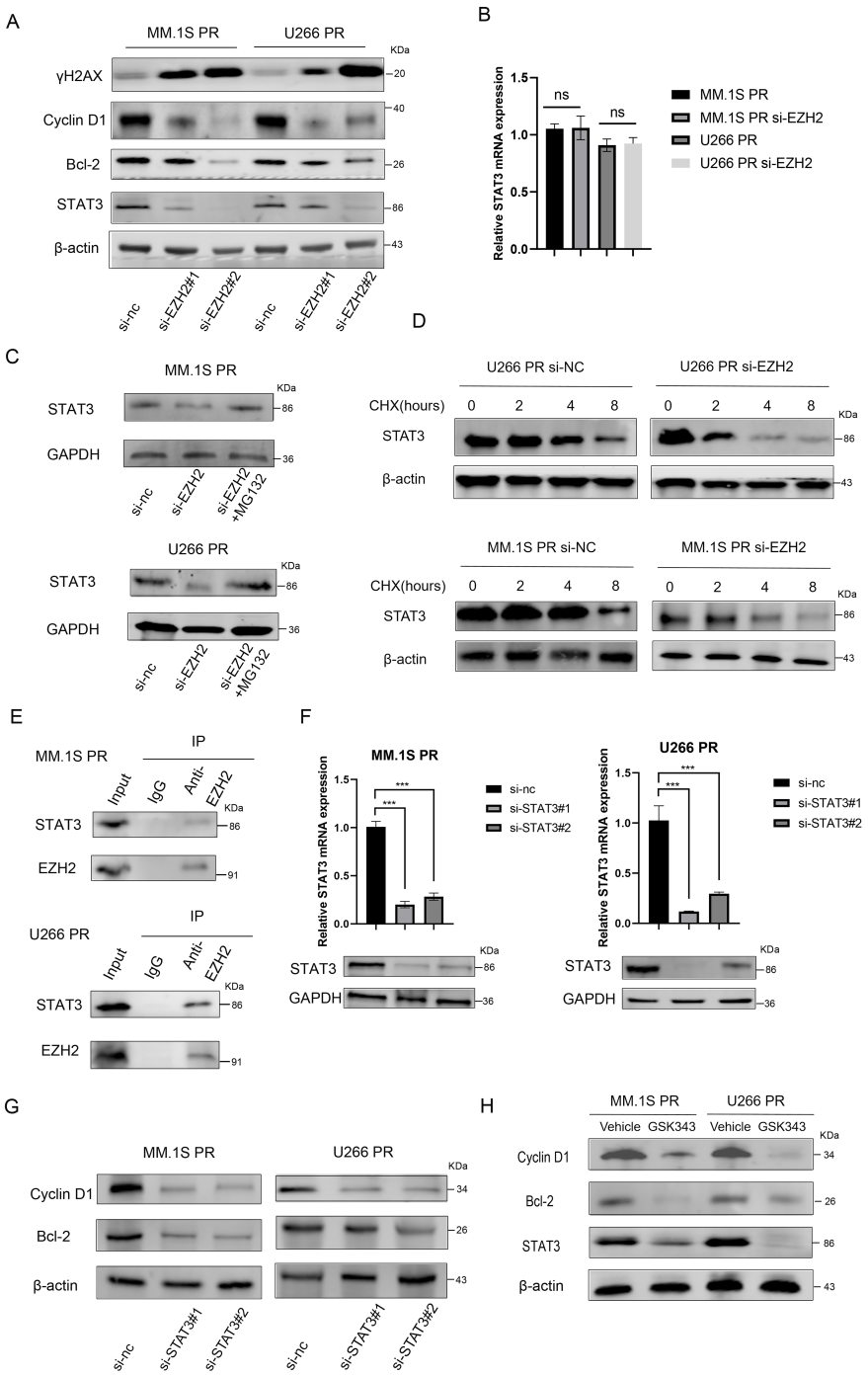


Figure 6. EZH2 stabilizes STAT3 protein to regulate apoptosis and the cell cycle in resistant MM cells (A) Western blot analysis showed that *EZH2* knockdown in pomalidomide-resistant MM cells reduced the levels of STAT3, Bcl-2, and Cyclin D1 and increased the level of the DNA damage marker γH2AX. (B) qPCR analysis showed that *EZH2* knockdown did not affect *STAT3* mRNA expression. (C) Proteasome inhibition with MG132 partially restored the STAT3 protein level in si-*EZH2*-treated resistant cells, indicating that EZH2 maintains STAT3 stability by protecting it from proteasome-mediated degradation. (D) Cycloheximide (CHX) chase analysis showing accelerated STAT3 protein turnover in pomalidomide-resistant MM cells following *EZH2* knockdown. Compared with siNC controls, si-*EZH2*-treated cells exhibited a more rapid decline in STAT3 protein levels after CHX treatment, indicating reduced STAT3 protein stability upon EZH2 depletion. (E) Co-IP analysis showing specific co-precipitation of STAT3 with EZH2, with this interaction consistently observed in both pomalidomide-resistant cell lines, indicating that EZH2 interacts directly with STAT3 to potentially regulate its stability. (F) *STAT3* knockdown (si-*STAT3*) at the mRNA and protein levels in resistant MM cells was validated by qPCR and western blot analysis, respectively. (G) Western blot analysis showed that *STAT3* knockdown recapitulated key downstream effects of *EZH2* silencing, including downregulation of Bcl-2 and Cyclin D1 but not γH2AX elevation, suggesting that EZH2 may regulate DNA repair independently of STAT3. (H) Pomalidomide-resistant MM.1S and U266 cells were treated with vehicle or GSK343, followed by western blot analysis. GSK343 treatment was associated with reduced STAT3 protein levels and decreased expression of the downstream markers Bcl-2 and Cyclin D1. Data are presented as the mean ± SD. ***$P < 0.001$; ns, not significant.

EZH2 sustains pomalidomide resistance primarily by stabilizing STAT3 protein, thereby maintaining STAT3-dependent Bcl-2 expression and cell cycle advancement to promote cell survival and proliferation. In parallel, EZH2 may independently enhance DNA repair capacity, providing additional protection against pomalidomide-induced stress. The upstream molecular determinants responsible for STAT3 stabilization, which potentially involve specific E3 ubiquitin ligases or deubiquitinases, remain to be clarified in future studies.

Discussion

Drug resistance remains a persistent challenge in MM, and the mechanisms underlying resistance to frontline IMiDs have drawn increasing attention [6,19]. Recent whole-genome sequencing analyses comparing paired samples from lenalidomide- and pomalidomide-treated RRMM patients with newly diagnosed cases identified EZH2 as a novel candidate driver gene in advanced disease, generating the need to understand its mechanistic role in drug resistance [15]. In this study, we identified EZH2 as a critical mediator of pomalidomide resistance in MM and demonstrated that both genetic depletion and pharmacologic inhibition of EZH2 could effectively restore the pomalidomide sensitivity of MM cells. Mechanistically, our experiments showed that EZH2 maintains resistance primarily by stabilizing STAT3 protein to sustain pro-survival and proliferative programs while also supporting DNA repair pathways that enable cells to tolerate pomalidomide-induced cytotoxic stress.

Our pharmacologic studies showed that targeting EZH2 could reverse pomalidomide resistance, underscoring the translational potential of this axis. The selective EZH2 inhibitor GSK343 reduced viability in both parental and resistant MM models. Comparable strategies targeting EZH2 enzymatic activity have shown efficacy in other models [20,21]. Genetic silencing of *EZH2* similarly suppressed tumor proliferation and partially restored pomalidomide sensitivity, reinforcing the functional role of EZH2 in pomalidomide resistance. These findings provide a rationale for ongoing clinical translation efforts, as the EZH2 inhibitor tazemetostat has already been approved for EZH2-driven malignancies, establishing a precedent for therapeutic targeting of EZH2 in cancer treatment [22,23].

We also tested the effects of the EZH2 PROTAC degrader MS1943. Unlike GSK343, MS1943 produced limited activity in parental cells and only partial effects in resistant cells in our experiments. Because GSK343 and MS1943 represent different therapeutic modalities (enzymatic inhibitor vs PROTAC degrader), the activity of these two compounds should not be overgeneralized to their entire classes. Instead, the observed discrepancy likely reflects compound-specific factors, such as ternary complex formation efficiency, E3 ligase recruitment compatibility, intracellular accumulation and stability, and the chromatin-associated context of EZH2 in specific cell states that govern degrader performance. These considerations are discussed in the primary literature on MS1943 and PROTAC design [24]. Importantly, the limited activity of a given PROTAC in a specific model does not exclude non-enzymatic roles of EZH2; rather, it highlights that robust evaluation of EZH2 depletion requires next-generation degraders optimized for bioavailability, appropriate E3 ligases, and chromatin access [25].

Notably, GSK343 not only showed greater cytotoxicity in resistant cells than its parental counterparts but also demonstrated clear synergy with pomalidomide in both *in vitro* and xenograft models. This cooperative activity suggests that EZH2 inhibition enhances pomalidomide efficacy under resistant conditions, supporting the translational relevance of EZH2 as both a predictive biomarker and a therapeutic co-target. Some preclinical studies, including an American Society of Hematology 2023 report showing that EZH2 inhibition followed by IMiD/CELMoD exposure reduces the viability of IMiD-resistant MM cell lines, suggest that EZH2 blockade may enhance IMiD efficacy in certain models [26,27]. Moreover, several EZH2-directed agents are currently in early-phase clinical evaluation (including tazemetostat and multiple investigational inhibitors), providing an actionable path for rapid clinical translation of combination approaches [22,28]. Taken together, these data support prioritizing the clinical testing of EZH2 modulation together with IMiD-based regimens in RRMM, ideally in biomarker-selected cohorts and with pharmacodynamic assessment to define optimal sequencing and dosing [29,30].

In the present study, resistant MM cells exhibited increases in both EZH2 and H3K27me3, a pattern previously linked to classical PRC2-mediated transcriptional repression in MM and other hematologic cancers [31–33]. Although this could suggest a canonical PRC2-dependent mechanism, RNA-seq profiling after *EZH2* knockdown in resistant MM cells revealed enrichment of broader pathways, including DNA damage responses, apoptosis, and cell cycle regulation, patterns that cannot be fully explained by H3K27me3 alone. These data raise the possibility that EZH2 contributes to pomalidomide resistance through noncanonical, methyltransferase-independent functions, consistent with reported PRC2-independent roles of EZH2 in regulating transcription, DNA repair, and signaling networks [13,34–36].

Although our transcriptomic analysis, together with established evidence linking the JAK-STAT pathway to myeloma biology and cell survival [37], identified this axis as a relevant candidate, our mechanistic studies focused specifically on STAT3 rather than the upstream signaling cascade [38,39]. This choice was guided by the observation that *EZH2* silencing sharply reduced STAT3 protein but not mRNA levels, implicating a post-transcriptional mechanism affecting protein stability. Mediation of STAT3 tyrosine phosphorylation by cytokine receptor engagement and subsequent activation of JAK kinases is well established [40], and because EZH2 is not known to regulate JAK kinases, direct activation of the canonical pathway by EZH2 is unlikely. Instead, our findings suggest that EZH2 stabilizes the STAT3 protein to maintain downstream pro-survival and proliferative signaling independent of upstream receptor input. Prior studies have shown that EZH2 can directly methylate STAT3 and thereby enhance STAT3 tyrosine phosphorylation and activity [41,42].

Previous research has characterized non-canonical STAT3 post-translational modifications that modulate its function [41]. Moreover, several studies have demonstrated that enhanced proteasome-mediated degradation of STAT3 can be reversed by treatment with the proteasome inhibitor MG132, indicating that decreases in STAT3 protein levels may reflect increased proteasomal turnover [43,44]. Together, these data provide a plausible mechanistic basis for our observation that *EZH2* knockdown reduced the STAT3 protein level without altering STAT3 mRNA expression. Additional studies have shown that EZH2 can regulate the protein stability of multiple partners via recruitment of deubiquitinases (*e.g.*, USP7) or by modulating ubiquitin-proteasome-related pathways, providing plausible molecular routes for EZH2-dependent stabilization of non-

histone proteins [45]. Consistent with proteasome-mediated regulation, proteasome inhibition was shown in multiple primary studies to rescue STAT3 protein levels after the induction of STAT3 degradation, supporting the interpretation that decreased STAT3 abundance can result from enhanced proteasomal turnover [46]. Together, these primary data establish credible mechanistic explanations for our finding that EZH2 maintains STAT3 protein stability via post-translational regulation.

The results of our functional experiments also align with this framework: *EZH2* knockdown reduced the STAT3 protein level, and proteasome inhibition partially restored STAT3 abundance, indicating proteasome-dependent regulation. Silencing of *STAT3* reproduced major downstream effects of EZH2 loss, including reduced Bcl-2 and Cyclin D1 levels, supporting a model in which the EZH2-STAT3 axis sustains anti-apoptotic and proliferative programs in resistant MM cells [47]. Parallel transcriptomic enrichment of DNA repair pathways and partial preservation of γH2AX changes after *STAT3* silencing indicate that EZH2 also influences DNA repair-related networks via STAT3-independent mechanisms [48], consistent with prior evidence that EZH2 participates in genomic maintenance beyond canonical histone methylation.

In the present study, pharmacologic inhibition of EZH2 only partially phenocopied the effects of genetic EZH2 depletion: while treatment with GSK343 led to a consistent downward trend in the levels of STAT3 protein and downstream markers, such decreases were not as pronounced as those observed after siRNA-mediated *EZH2* knockdown. This partial concordance suggests that while the catalytic methyltransferase activity of EZH2 likely contributes to STAT3 maintenance, non-catalytic functions of EZH2, such as protein-protein interaction, structural scaffolding, or control of post-translational modifications, may play a significant role. Indeed, previous work in glioblastoma stem-like cells demonstrated that EZH2 binds to and methylates STAT3, enhancing its tyrosine phosphorylation and transcriptional activity, and inhibition or genetic silencing of EZH2 substantially reduces STAT3 activation in these cells [49,50]. Likewise, in breast cancer models, EZH2 suppression diminishes STAT3 nuclear localization and target gene activation, impairing proliferation and migration [51]. These findings support a model in which EZH2 coordinates canonical (methyltransferase-dependent) and noncanonical functions that sustain STAT3 protein stability and downstream signaling in drug-resistant MM cells.

Recent studies have highlighted multiple therapeutic strategies targeting EZH2 in multiple myeloma, including not only selective EZH2 inhibitors but also combinatorial approaches such as dual DNMT/EZH2 inhibition, which have demonstrated enhanced anti-tumor activity through coordinated epigenetic reprogramming [27]. Compared with these strategies, our findings emphasize a distinct mechanism whereby EZH2 contributes to pomalidomide resistance through stabilization of STAT3, suggesting that targeting EZH2 may exert both epigenetic and non-canonical regulatory effects in resistant MM cells.

Notably, we employed both enzymatic inhibition and targeted protein degradation approaches and observed consistent anti-proliferative effects in resistant cells, supporting the functional relevance of EZH2 targeting. However, it is important to acknowledge that PROTAC-based degraders such as MS1943 may face limitations in clinical translation, including suboptimal bioavailability and pharmacokinetic properties [24]. Therefore, while our results support EZH2 as a promising therapeutic target, further optimization of drug design and evaluation in clinically relevant models will be necessary before broad generalization of these findings.

Despite the compelling evidence presented, several limitations remain in this study. First, although our data strongly support a role for EZH2 in stabilizing STAT3 protein, the specific E3 ubiquitin ligases or deubiquitinases involved remain unidentified. Second, while GSK343 serves as a valuable tool compound, it is not clinically optimized; therefore, future work should evaluate next-generation EZH2 inhibitors or degraders with improved pharmacokinetic properties. Finally, although our study utilized patient-derived RRMM samples, larger cohorts and clinical trials will be necessary to validate EZH2 as a therapeutic target and predictive biomarker in diverse patient populations.

Future work should aim to identify the E3 ubiquitin ligases or deubiquitinases mediating STAT3 stabilization, delineate the interplay between EZH2's catalytic and non-catalytic functions, determine biomarkers that could guide patient stratification for EZH2-targeted therapies, and analyze how EZH2 integrates into broader regulatory networks that govern MM evolution under therapeutic pressure.

In summary, based on integrated transcriptomic, biochemical, and pharmacologic evidence, we propose that EZH2 contributes to the pomalidomide resistance of MM through dual modalities, epigenetic repression via PRC2 and post-translational stabilization of STAT3, which promotes MM survival and cell cycle progression and supports DNA repair processes that mitigate drug-induced damage. Our findings provide a mechanistic rationale for the clinical evaluation of EZH2-targeting strategies, alone or in combination with IMiDs, in RRMM.

Supplementary Data

Supplementary data are available at *Acta Biochimica et Biophysica Sinica* online.

Data Availability

The data supporting the findings of this study can be found in the article, Supplementary Information, or available from the corresponding author upon reasonable request. The raw sequencing data generated in this study have been deposited in the NCBI Gene Expression Omnibus (GEO) database under accession number GSE317666.

Author Contributions

Xiaohui Zhang designed the research and contributed reagents and other essential materials. Xinyuan Zhang performed the research. Ruijing Hu, Kexin Hu, Qi Li, Linlin Qin, and Yali Chai modified the paper. Wenzhuo Zhuang provided guidance on the analysis and interpretation of sequencing data.

Acknowledgement

We thank Medjaden Inc. (Wuhan, China) for scientific editing of this manuscript.

Funding

This work was supported by the grant from the Top-notch Young Health Talents, and the 5th Suzhou Health Professionals Program (No. GSWS2020027 to X.H.Z.).

Conflict of Interest

The authors declare that they have no conflict of interest.

References

1. Rajkumar SV. Multiple myeloma: 2020 update on diagnosis, risk-stratification and management. *Am J Hematol* 2020, 95: 548–567
2. Kumar SK, Rajkumar V, Kyle RA, van Duin M, Sonneveld P, Mateos MV, Gay F, *et al.* Multiple myeloma. *Nat Rev Dis Primers* 2017, 3: 17046
3. Miguel JS, Weisel K, Moreau P, Lacy M, Song K, Delforge M, Karlin L, *et al.* Pomalidomide plus low-dose dexamethasone versus high-dose dexamethasone alone for patients with relapsed and refractory multiple myeloma (MM-003): a randomised, open-label, phase 3 trial. *Lancet Oncol* 2013, 14: 1055–1066
4. Holstein SA, McCarthy PL. Immunomodulatory drugs in multiple myeloma: mechanisms of action and clinical experience. *Drugs* 2017, 77: 505–520
5. Ntanasis-Stathopoulos I, Malandrakis P, Filippatos C, Maganas S, Fotiou D, Theodorakakou F, Spiliopoulou V, *et al.* Pomalidomide, cyclophosphamide, and dexamethasone for relapsed/refractory multiple myeloma: a single-center experience. *Clin Lymphoma Myeloma Leuk* 2025, 25: e1077–e1085
6. Patel R, Patel D, Patel Z, Patel M, Chitkara A, Yang C, Onyechi A, *et al.* Disparities in palliative care utilization in deceased lymphoma patients: a nationwide analysis. *Blood* 2023, 142: 131
7. Krönke J, Udeshi ND, Narla A, Grauman P, Hurst SN, McConkey M, Svinkina T, *et al.* Lenalidomide causes selective degradation of IKZF1 and IKZF3 in multiple myeloma cells. *Science* 2014, 343: 301–305
8. van de Donk NWCJ, Bahlis NJ, Pawlyn C, Gay F, Mateos MV, Weisel K, Lonial S, *et al.* The role of CELMoD agents in multiple myeloma. *Onco Targets Ther* 2025, 18: 921–933
9. Touzeau C, Lipe B, Khan AM, Dhakal B, Nair S, He J, Mendes J, *et al.* Comparative effectiveness of ciltacabtagene autoleucel in CARTITUDE-4 versus real-world physician's choice of therapy from the flatiron registry in lenalidomide-refractory multiple myeloma. *Adv Ther* 2025, 42: 5023–5041
10. Margueron R, Reinberg D. The polycomb complex PRC2 and its mark in life. *Nature* 2011, 469: 343–349
11. Kim KH, Roberts CWM. Targeting EZH2 in cancer. *Nat Med* 2016, 22: 128–134
12. Verma S, Goyal N, Goyal S, Kaur P, Gupta S. EZH2 dysregulation and its oncogenic role in human cancers. *Cancers* 2025, 17: 3111
13. Pawlyn C, Bright MD, Buros AF, Stein CK, Walters Z, Aronson LI, Mirabella F, *et al.* Overexpression of EZH2 in multiple myeloma is associated with poor prognosis and dysregulation of cell cycle control. *Blood Cancer J* 2017, 7: e549
14. Knutson SK, Kawano S, Minoshima Y, Warholic NM, Huang KC, Xiao Y, Kadowaki T, *et al.* Selective inhibition of EZH2 by EPZ-6438 leads to potent antitumor activity in *EZH2*-mutant non-Hodgkin lymphoma. *Mol Cancer Ther* 2014, 13: 842–854
15. Ansari-Pour N, Samur M, Flynt E, Gooding S, Towfic F, Stong N, Estevez MO, *et al.* Whole-genome analysis identifies novel drivers and high-risk double-hit events in relapsed/refractory myeloma. *Blood* 2023, 141: 620–633
16. Zayad A, Magee G, Mansour R, Chang M, Ahmed N, Mushtaq MU, Paul B, *et al.* Efficacy and safety of daratumumab, pomalidomide and dexamethasone compared to daratumumab, carfilzomib and dexamethasone in relapsed multiple myeloma: multicenter real-world experience. *Clin Lymphoma Myeloma Leukemia* 2026, 26: 94–105
17. Boccadoro M, Belotti A, Bombaci F, Bringhen S, Buda G, Cafro AM, Caimmi M, *et al.* Supporting treatment decision-making for patients with multiple myeloma post-DRd in Italy: a multi-criteria decision framework. *BMC Cancer* 2025, 25: 1676
18. Yi JH, Park SS, Min CK, Lee JH, Eom HS, Lee JH, Kim K. Carfilzomib, pomalidomide, and dexamethasone for multiple myeloma after carfilzomib, lenalidomide, and dexamethasone. *Int J Hematol* 2026, 123: 263–269
19. Zamagni E, Barbato S, Cavo M. How I treat high-risk multiple myeloma. *Blood* 2022, 139: 2889–2903
20. Yu T, Wang Y, Hu Q, Wu WN, Wu Y, Wei W, Han D, *et al.* The EZH2 inhibitor GSK343 suppresses cancer stem-like phenotypes and reverses mesenchymal transition in glioma cells. *Oncotarget* 2017, 8: 98348–98359
21. Sbirkov Y, Schenk T, Kwok C, Stengel S, Brown R, Brown G, Chesler L, *et al.* Dual inhibition of EZH2 and G9A/GLP histone methyltransferases by HKMTI-1-005 promotes differentiation of acute myeloid leukemia cells. *Front Cell Dev Biol* 2023, 11: 1076458
22. Straining, PharmD R, Eighmy, PharmD W. Tazemetostat: EZH2 inhibitor. *JADPRO* 2022, 13: 158–163
23. Yang X, Xu L, Yang L. Recent advances in EZH2-based dual inhibitors in the treatment of cancers. *Eur J Med Chem* 2023, 256: 115461
24. Ma A, Stratikopoulos E, Park KS, Wei J, Martin TC, Yang X, Schwarz M, *et al.* Discovery of a first-in-class EZH2 selective degrader. *Nat Chem Biol* 2020, 16: 214–222
25. Tang M, Gong M, Liu X, Zhang T, Liu Z, Song D. Recent update on the development of EZH2 inhibitors and degraders for cancer therapy. *Eur J Med Chem* 2025, 299: 118106
26. Herviou L, Kassambara A, Boireau S, Robert N, Requirand G, Müller-Tidow C, Vincent L, *et al.* PRC2 targeting is a therapeutic strategy for EZ score defined high-risk multiple myeloma patients and overcome resistance to IMiDs. *Clin Epigenet* 2018, 10: 121
27. Dimopoulos K, Søgaard Helbo A, Fibiger Munch-Petersen H, Sjö L, Christensen J, Sommer Kristensen L, Asmar F, *et al.* Dual inhibition of DNMTs and EZH2 can overcome both intrinsic and acquired resistance of myeloma cells to IMiDs in a cereblon-independent manner. *Mol Oncol* 2018, 12: 180–195
28. Morschhauser F, Tilly H, Chaidos A, McKay P, Phillips T, Assouline S, Batlevi CL, *et al.* Tazemetostat for patients with relapsed or refractory follicular lymphoma: an open-label, single-arm, multicentre, phase 2 trial. *Lancet Oncol* 2020, 21: 1433–1442
29. Tremblay-LeMay R, Rastgoo N, Pourabdollah M, Chang H. EZH2 as a therapeutic target for multiple myeloma and other haematological malignancies. *Biomark Res* 2018, 6: 34
30. Dimopoulos MA, Leleu X, Palumbo A, Moreau P, Delforge M, Cavo M, Ludwig H, *et al.* Expert panel consensus statement on the optimal use of pomalidomide in relapsed and refractory multiple myeloma. *Leukemia* 2014, 28: 1573–1585
31. Hernando H, Gelato KA, Lesche R, Beckmann G, Koehr S, Otto S, Steigemann P, *et al.* EZH2 inhibition blocks multiple myeloma cell growth through upregulation of epithelial tumor suppressor genes. *Mol Cancer Ther* 2016, 15: 287–298
32. Liu R, Li Z, Chen R, Fang Z, Liu Z, Liu H. EZH2 serves as a viable therapeutic target for myeloma-induced osteolytic bone destruction. *Nat Commun* 2025, 16: 1206
33. Ting PY, Borikar S, Kerrigan JR, Thomsen NM, Aghania E, Hinman AE, Pizzato N, *et al.* Targeted degradation of the Wiz transcription factor for gamma globin de-repression. *Blood* 2023, 142: 2
34. Kim J, Lee Y, Lu X, Song B, Fong KW, Cao Q, Licht JD, *et al.* Polycomb- and methylation-independent roles of EZH2 as a transcription activator. *Cell Rep* 2018, 25: 2808–2820.e4
35. Wang J, Wang GG. No easy way out for EZH2: its pleiotropic,

noncanonical effects on gene regulation and cellular function. *Int J Mol Sci* 2020, 21: 9501

36. Xu L, Tang H, Wang K, Zheng Y, Feng J, Dong H, Jin Y, ***et al.*** Pharmacological inhibition of EZH2 combined with DNA-damaging agents interferes with the DNA damage response in MM cells. *Mol Med Report* 2019
37. Lu C, Talukder A, Savage NM, Singh N, Liu K. JAK-STAT-mediated chronic inflammation impairs cytotoxic T lymphocyte activation to decrease anti-PD-1 immunotherapy efficacy in pancreatic cancer. *OncoImmunology* 2017, 6: e1291106
38. Yu H, Pardoll D, Jove R. STATs in cancer inflammation and immunity: a leading role for STAT3. *Nat Rev Cancer* 2009, 9: 798–809
39. Yu H, Kortylewski M, Pardoll D. Crosstalk between cancer and immune cells: role of STAT3 in the tumour microenvironment. *Nat Rev Immunol* 2007, 7: 41–51
40. Gleisner AL, Moss A, Friedman C, Suresh K, Grunwald G, Torphy RJ, Leonard LD, ***et al.*** De-implementation of axillary dissection in women with breast cancer is largely driven by site-level contextual effects. *Ann Surg* 2022, 276: e923–e931
41. Dasgupta M, Dermawan JKT, Willard B, Stark GR. STAT3-driven transcription depends upon the dimethylation of K49 by EZH2. *Proc Natl Acad Sci USA* 2015, 112: 3985–3990
42. Müller A, Dickmanns A, Resch C, Schäkel K, Hailfinger S, Dobbelstein M, Schulze-Osthoff K, ***et al.*** The CDK4/6-EZH2 pathway is a potential therapeutic target for psoriasis. *J Clin Invest* 2020, 130: 5765–5781
43. Wu Z, Liu H, Sun W, Du Y, He W, Guo S, Chen L, ***et al.*** RNF180 mediates STAT3 activity by regulating the expression of RhoC via the proteasomal pathway in gastric cancer cells. *Cell Death Dis* 2020, 11: 881
44. Qu X, Ma W, Ma X, Liu J, Yang X, He D, Sun Y. Study on the mechanism of aspirin alleviating Kawasaki disease with coronary artery lesions by inducing TRAF6 to regulate STAT3 ubiquitination and inhibit Th17 cell differentiation. *Drug Dev Res* 2025, 86: e70199
45. Lei A, Chen L, Zhang M, Yang X, Xu L, Cao N, Zhang Z, ***et al.*** EZH2 regulates protein stability via recruiting USP7 to mediate neuronal gene expression in cancer cells. *Front Genet* 2019, 10: 422
46. Yang L, Wang R, Ma Z, Xiao Y, Nan Y, Wang Y, Lin S, ***et al.*** Porcine reproductive and respiratory syndrome virus antagonizes JAK/STAT3 signaling via nsp5, which induces STAT3 degradation. *J Virol* 2017, 91: e02087-16
47. Kujawski M, Zhang C, Herrmann A, Reckamp K, Scuto A, Jensen M, Deng J, ***et al.*** Targeting STAT3 in adoptively transferred T cells promotes their *in vivo* expansion and antitumor effects. *Cancer Res* 2010, 70: 9599–9610
48. Wang X, He M, Zhou L, Chen W. EZH2 expression in hepatocellular carcinoma and its relationship with circadian rhythm-related genes. *Sci Rep* 2025, 15: 42177
49. Kim E, Kim M, Woo DH, Shin Y, Shin J, Chang N, Oh YT, ***et al.*** Phosphorylation of EZH2 activates STAT3 signaling via STAT3 methylation and promotes tumorigenicity of glioblastoma stem-like cells. *Cancer Cell* 2013, 23: 839–852
50. Gan L, Yang Y, Li Q, Feng Y, Liu T, Guo W. Epigenetic regulation of cancer progression by EZH2: from biological insights to therapeutic potential. *Biomark Res* 2018, 6: 10
51. Zhao Y, Hu Z, Li J, Hu T. EZH2 exacerbates breast cancer by methylating and activating STAT3 directly. *J Cancer* 2021, 12: 5220–5230